AJNR

Dynamic Spin Labeling Angiography in Extracranial Carotid Artery Stenosis

Carsten Warmuth, Maria Rüping, Annette Förschler, Hans-Christian Koennecke, Jose Manuel Valdueza, Andreas Kauert, Stephan J. Schreiber, Ralf Siekmann and Claus Zimmer

Dynamic Spin Labeling Angiography in Extracranial Carotid Artery Stenosis

Carsten Warmuth, Maria Rüping, Annette Förschler, Hans-Christian Koennecke, Jose Manuel Valdueza, Andreas Kauert, Stephan J. Schreiber, Ralf Siekmann, and Claus Zimmer

BACKGROUND AND PURPOSE: Similar to digital subtraction angiography, dynamic spin labeling angiography (DSLA) provides time-resolved measurements of the influx of blood into the cerebral vascular tree. We determined whether DSLA may help in assessing the degree of stenosis and whether it provides information about intracerebral collateralization and allows us to monitor the hemodynamic effects of vascular interventions.

METHODS: We developed a segmented DSLA sequence that allowed the formation of images representing inflow delays in 41-ms increments. Thirty patients with unilateral carotid artery stenosis and 10 control subjects underwent DSLA. Arrival times of the labeled arterial blood bolus were measured in the carotid siphon (CS) and the middle cerebral artery (MCA) on both sides, and the corresponding side-to-side arrival time differences (ATDs) were calculated. ATDs before and after carotid endarterectomy or percutaneous angioplasty were studied in 10 patients.

RESULTS: The degree of stenosis was significantly correlated with ATD in the cerebral vessels. Receiver operating characteristic analysis yielded a cutoff CS ATD of 110 ms to separate stenoses <70% from those ≥70%, with a sensitivity of 90% and a specificity of 67%. In one third of patients, ATD was higher in the MCA than in the CS; this finding suggested an absence of collateralization. Most patients had reduced ATD in the MCA. The degree of ATD reduction was regarded as a quantitative measure of collateralization. Successful intervention resulted in normalized ATDs.

CONCLUSION: DSLA is a promising method that allowed us to noninvasively quantify the hemodynamic effect of extracranial carotid stenosis and the resulting intracranial collateralization.

Current CT- and MR imaging-based angiographic techniques provide high spatial resolution. Combined with Doppler ultrasonography, they allow us to precisely determine the degree of extracranial internal carotid artery (ICA) stenoses (1). The results are closely correlated with those of digital subtraction angiography DSA. However, both MR and CT angiography are limited by a relatively low temporal resolution on the order of several seconds. With this

limitation, it is nearly impossible to directly assess the collateralization of an ischemic area from primarily unaffected vascular territories. However, indirect information can be obtained. Supplementary to morphologic measurement of the site, length and lumen of a stenosis, contrast-enhanced dynamic MR or CT imaging provides physiologic and hemodynamic information. Regional tissue perfusion deficits associated with occlusive cerebrovascular disease can be demonstrated by using these techniques. Impaired autoregulation was found in patients with carotid artery stenosis by analyzing cerebral blood flow maps before and after acetazolamide stimulation (2). Another study showed a significant relation between hemispheric mean transit time and the degree of collateralization, as seen on DSA (3). In the circle of Willis, phase-contrast MR angiography (MRA) can be used to depict the direction of blood flow and its changes over time without the use of contrast agents (4). Nevertheless, the lack of adequate information on collateralization is an important reason why DSA is still used in patients with extracranial stenoses of
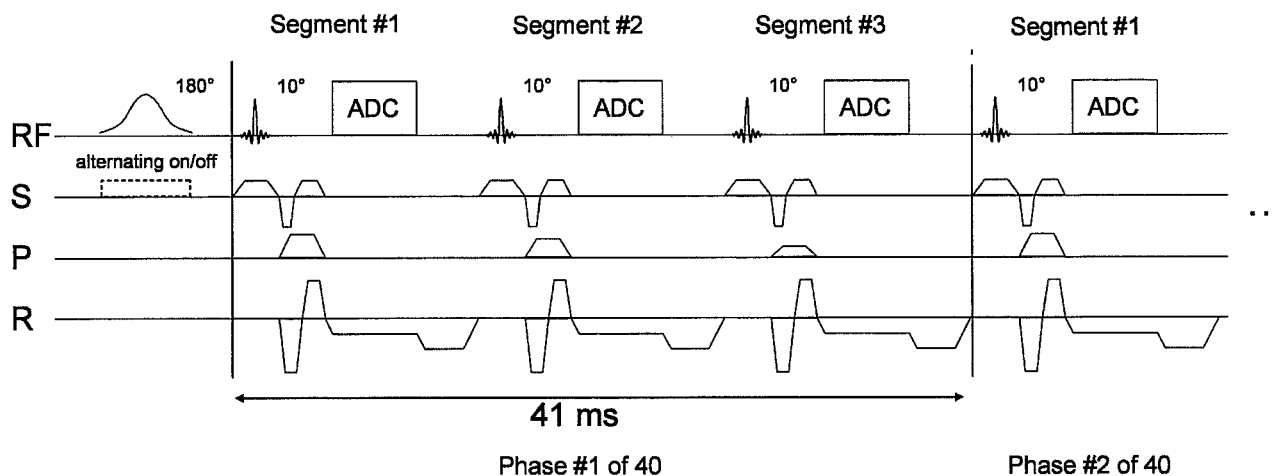
FIG 1. DSLA sequence scheme. After the section selective/nonselective labeling pulse, multiphase data acquisition started in a cine-like fashion. Any segmentable gradient-echo readout may be used. Figure depicts FLASH readout with threefold segmentation and flow compensation in the section and read directions. ADC indicates analog-to-digital converter; RF, radio frequency; S, section direction gradient.

the carotid or vertebral arteries despite the invasiveness of this technique and the occurrence of postprocedural diffusion disturbances in up to 10% (5).

In the present study, we addressed whether MR spin labeling is useful for evaluating hemodynamic changes associated with stenosing cerebrovascular disease. With a number of MR techniques, spin labeling is used to visualize blood flow noninvasively. In spin labeling, the magnetization of inflowing blood is prepared by using inversion or saturation pulses, which make it distinguishable from static tissue. The altered magnetization decays within a few seconds, but this time suffices to quantify blood flow in tissue (6). Most studies have focused on flow on the capillary level to assess tissue perfusion (e.g., with functional MR imaging) or to determine local organ perfusion, such as that of the kidney or the heart. Various techniques are used to specifically suppress the blood signal intensity from the arteries (e.g., by applying flow-sensitive gradients or by saturating the distal end of the labeled blood bolus in combination with delayed image acquisition) (7). Although spin labeling was show to be suitable for visualizing vessels on projection angiograms by using pulsed (8, 9) or continuous inversion (10), it is rarely used for angiography because time-of-flight or contrast-enhanced MRAs are of higher quality and, more important, 3D at identical acquisition times.

We present a DSLA technique characterized by a particularly high temporal resolution. The basic approach is to vary the inversion delay in pulsed spin-labeling angiography, as described in the early 1990s (11, 12). To our knowledge, no group has investigated the use of this technique for analyzing changes in cerebral blood flow dynamics in patients with extracranial vascular stenoses. We optimized DSLA for clinical use by introducing segmented data acquisition to shorten the acquisition time at the expense of temporal resolution. The selection of a combination of acquired lines, bandwidth, and segmentation allowed us to adjust the temporal and spatial resolution, as well as the acquisition time, over wide ranges.

The purpose of the present study was to determine whether this technique is suitable for determining the degree of stenosis in patients with extracranial carotid artery stenoses by precise analysis of arrival time differences (ATDs). In addition and probably more important, the investigation addressed the issue of whether DSLA provides information about intracerebral collateralization and whether it allows us to monitor the hemodynamic effects of interventional vascular procedures.

Methods

DSLA Technique

DSLA is based on the same principle as DSA. In DSA, contrast medium is injected directly into an artery through a catheter, and its distribution is visualized on a series of radiographs acquired in rapid succession. For analysis, the nonenhanced fluoroscopic image is digitally subtracted from the subsequent images to eliminate the background signal intensity of static tissue. In spin labeling angiography, the contrast medium is replaced by magnetic labeling of the blood, which is done at a defined point in time (pulsed spin labeling) (13, 14). As with DSA, control images without labeling are obtained and subtracted, leaving only the blood signal intensity. A quasi-dynamic study can be done by varying the delay (i.e., TI) between labeling and image acquisition (12).

We used the flow alternating inversion-recovery (FAIR) labeling scheme (15, 16). With FAIR, label and control images were acquired after global and section-selective inversion, respectively. This scheme had the advantage of labeling all blood in the transmitter coil and precluding subtraction errors due to magnetization transfer. We implemented hyperbolic secant inversion pulses that provided a good section profile and made the inversion almost insensitive to B_1 inhomogeneities. Figure 1 illustrates the technique of DSLA. Instead of acquiring data in a single temporal window with a varying postlabeling delay, multiple time steps were sampled in cine-like fashion by using gradient-echo data acquisition with a small excitation flip angle. This principle of simultaneously sampling multiple inversion times was first introduced by Look and Locker for fast T1

determination (17). It is clear from Figure 1 that the readout length and the number of segments N determine the temporal resolution. After the acquisition of the N identical k-space lines for all phases after global inversion, time was given to allow for decay and complete washout of labeled blood from the section. Subsequently, the same readout train acquired N k-space lines of the control images following section selective inversion. With M lines to measure for a complete image, acquisition of a data set was finished after 2·M/N inversion pulses.

However, DSLA and DSA have several differences. First and most important, magnetic labeling is subject to relaxation and can only be traced for a short period of 1 to 2 seconds. Second, the excitation pulses used for image acquisition accelerate relaxation and thereby destroy the labeling effect. Imaging with a flip angle of 90° completely excites longitudinal magnetization in the imaging plane and fully exploits the labeling effect, but does not allow for repetitive acquisition in multiple phases. By using a smaller excitation angle, data can be acquired in multiple phases after a single blood inversion. However, with a decreased measuring signal intensity compared with a single phase measurement. Nevertheless, the overall signal-to-noise ratio of such an image series is higher than that of several images acquired individually (18). Third, to achieve high temporal resolution with DSLA, only some k-space lines of each image in the series are measured after one magnetization preparation. The dynamic study thus comprises data acquired in a large number of repeated labeling experiments. This procedure requires blood flow dynamics to be the same after each magnetization, which is why ECG triggering should be used.

Patients and Subjects

The study was approved by the institutional review board, and informed consent was obtained from all participants. As a control group, 10 healthy subjects (three men, seven women; age range, 53–80 years; mean age, 67 years) were examined. The absence of stenotic lesions of extracranial and intracranial brain arteries was confirmed with extracranial and transcranial ultrasonography. Thirty patients (16 men, 14 women; age range 50–80 years; mean age, 67 years)) with unilateral extracranial stenoses of the ICA were examined. The degree of stenosis was determined (C.W., C.Z.) on DSA in 18 patients by using the North American Symptomatic Carotid Endarterectomy Trial (NASCET) method (19). In the other 12 patients, two independent examiners (J.M.V., S.J.S.) determined the degree with extracranial duplex sonography, according to standard European Carotid Surgery Trial (ECST) criteria (20). These results were converted into NASCET values (21). The average interval between assessment of the degree of stenosis and MR imaging was 4 days, with a maximum of 22 days.

ICA stenosis was symptomatic in 22 patients and asymptomatic in eight. Among the patients with symptomatic stenosis, 17 had had a cerebral infarction, and five had presented with a TIA within 4 weeks preceding the examination. In two symptomatic patients, cerebral infarction was older than 28 days. Ten of the patients underwent repeat imaging after either carotid endarterectomy ($n = 6$) or angioplasty with stent placement ($n = 4$). The maximum interval between carotid endarterectomy or stent angioplasty and imaging was 11 days; the average was 8 days. Patients with additional extracranial or intracranial vascular stenoses on the contralateral side were not included in the study.

Study Protocol

All examinations were performed by using a 1.5-T wholebody MR imager (Magnetom Vision, Siemens Erlangen, Germany) with the transmit/receive head coil. Three-lead ECG (Bruker, Rheinstetten, Germany) with active amplification was used for triggering. Proton density- and T2-weighted axial images of the entire brain were acquired by using a double-echo turbo spin-echo sequence (TR/TE1/TE2 = 3800/22/90, turbo factor of 5, flip angle of 90°), followed by time-of-flight MRA of the intracranial vessels by using a gradient-echo sequence (TR/TE = 22/5.3, flip angle of 20°).

Intracerebral flow was studied by using a matrix of 192 × 256 (6/8 230-mm field of view), resulting in 128 inversion pulses. With an interval of 2500 ms between two inversion pulses, the minimum acquisition time was 5 minutes 20 seconds. A triply segmented flow-compensated gradient-echo sequence (FLASH) was used with a TE of 6.1 ms, a bandwidth of 195 Hz per pixel, and a temporal resolution of 41 ms or 25 images per second. This was adequate for visualizing the rapid blood flow in the cerebral arteries. Use of a flip angle of 10° allowed us to track the labeled blood on a series of 40 images, covering an interval of 0 to 1640 ms.

Two ECG-triggered DSLA acquisitions with different section thicknesses (40 and 30 mm) were performed, one at the level of the circle of Willis and one at the level of the carotid siphon (CS). Both acquisitions were performed in the transverse orientation depicting the vessels in head-to-foot projection. By using FAIR, blood entering the imaging section from above (e.g., in the sagittal and transverse sinuses) was likewise visualized, but this was not a problem in a transverse projection. It was important for labeling to be performed distal to the stenosis, as the label was not imaged while passing through it. Consequently, possible passage delays did not contribute to the arrival time, and instead slower flow or late filling through the circle of Willis was solely responsible.

Analysis

Movie sequences showing cerebral blood arrival were generated from each examination for a qualitative analysis of cerebral blood flow and visual assessment of collateralization, which was rated in the following way: High collateral flow was assigned to patients with bright connecting vessels and a distinct directionality of blood flow to the affected hemisphere. Low collateral flow meant less prominent collaterals. Assessment was rated inconclusive in case of low vessel signal intensity or if the temporal resolution was insufficient to determine the flow direction.

For quantitative analysis, arrival of magnetized blood was measured in control subjects and in patients on both sides at two sites: proximal to the origin of the ophthalmic artery in the DSLA obtained at the level of the CS and at the bifurcation of the MCA in the DSLA obtained at the level of the circle of Willis. Figure 2 depicts such signal intensity time courses measured in the MCA of a patient. They were normalized to their respective maximum for comparison. For precise determination of arterial arrival, the time at which the signal intensity reached 50% of the maximal amplitude was measured on both sides. The temporal resolution was virtually increased by linear interpolation between points, thus signal intensities were used to a certain extent to improve ATD accuracy. Arrival times were determined on a 10-ms time scale instead of the 41 ms originating from the acquisition. In the group of patients, absolute arrival times and ipsilateral and contralateral ATDs were determined. In the control group, right-side measurements were subtracted from left-side measurements, yielding the ATD.

Statistical analysis was performed by using SPSS (SPSS Inc., Chicago, IL). The degree of stenosis and the ATDs were tested for statistically significant correlations by using a nonparametric test according to Kendall. Groups were defined (controls, stenoses <70% and ≥70%) and compared for statistically significant ATD differences by using a Mann-Whitney nonparametric test. Significance was assumed at $P < .05$. A receiver operating characteristic (ROC) analysis was performed to assess sensitivity and specificity of group discrimination on the basis of calculated ATDs. The optimal cutoff value for maximizing the product of sensitivity and specificity and that for 100% specificity were determined.
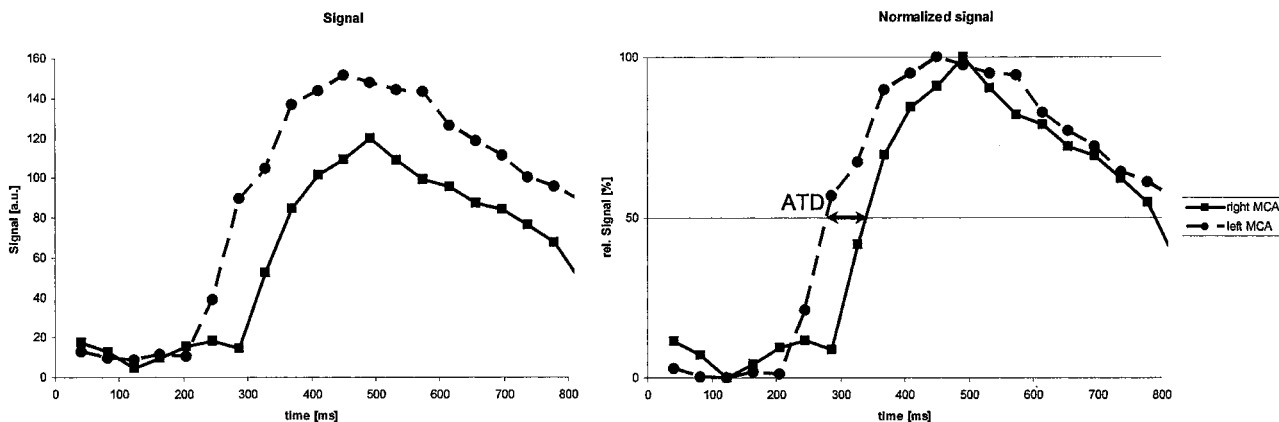
FIG 2.   Determination of ATDs. *Left*, Original signal intensity–time courses measured in the left and right MCAs. *Right*, Normalized curves (divided by the respective maximum value). By using linear interpolation between the measured points, the intersection at which the signals reached 50% was determined. Difference was referred to as the ATD (*arrows*).

TABLE 1: Quantitative results in the control group

Subject	ATD (msec)	
	CS	MCA
1	30	10
2	10	20
3	20	20
4	10	20
5	30	−20
6	0	40
7	20	30
8	20	30
9	20	30
10	0	0
All*	16 ± 11	19 ± 17

*Data are the mean ± standard deviation.

Results

In contrast to the analysis of ATDs, evaluation of absolute arrival times yielded no meaningful results. Tables 1 and 2 summarize the data on control subjects and patients, respectively. Listed are the degree of stenosis determined on DSA or duplex ultrasonography and ATDs of arterial blood in the CS and the MCA. In two patients with 95% stenosis, no blood signal intensity could be detected in the CS.

Control group

The average ATD between the right and left side in the control group was 16 ms at the level of the CS and 19 ms at the level of the MCA. The greatest differences between the right and left side were 30 and 40 ms, respectively.

Patients

Qualitative analysis of DSLA.—DSLA, in particular, allowed for good qualitative assessment of collateralization via the circle of Willis, i.e., whether collateral flow occurs mainly through the anterior communicating artery from the contralateral hemisphere or rather from the ipsilateral posterior terri-

tory via the posterior communicating artery. Figure 3 shows images from a patient with pronounced collateral flow via the circle of Willis. In one patient, retrograde flow in the ophthalmic artery and leptomeningeal collaterals were clearly depicted in the DSLA image series.

Quantitative Analysis of ATDs.—The degree of stenosis was clearly related to the ATDs calculated for the CS and for the MCA (Fig 4). The correlation is statistically significant for both sites of measurement ($P < .01$). For further evaluation, the subjects were subdivided into three groups, according to their degree of stenosis: 0% (controls), <70% and ≥70%. ATDs in the CS and MCA were significantly different between the control group and patients with stenoses ≥70%, as well as between patients with ≥70% and those with <70% stenosis. The only factor that significantly differed between control subjects and patients with stenoses <70% was ATD in the CS. By using ROC analysis, cutoff values were determined to predict the classification of each patient into either of the groups with highest specificity and sensitivity. Because the ATD values at the CS level were of highest significance regarding the degree of stenosis, only these were used in the ROC analysis. Figure 5 depicts the ROC curves. The optimal cutoff value separating controls and stenoses <70% was 35 ms (sensitivity, 80%; specificity, 100%). The cutoff separating stenoses <70% from those ≥70% was 110 ms (sensitivity, 67%; specificity, 90%). Transit time delays of more than 150 ms in the CS are indicative for high-grade stenoses (sensitivity, 56%; specificity, 100%).

Figure 6 shows a scatterplot of the individual ATDs proximal and distal to the circle of Willis of all patients, grouping them according to the visually rated poststenotic collateral flow. The degree of collateralization visible in the circle of Willis was correlated with the ATD CS/ATD MCA ratio, with a higher degree of collateralization associated with reduced distal ATDs. No interrelation could be found between the patients' clinical picture (asymptomatic, TIA, or infarction) and the degree of collateralization.

TABLE 2: Quantitative results in patients

Patient	Degree of Stenosis (%)	ATD (msec)			
		CS	CS, After Surgery	MCA	MCA, After Surgery
11	30	40		10	
12	30	20		−100	
13	30	100		110	
14	30	40		10	
15	30	30		−30	
16	50	40		40	
17	50	80	10	30	20
18	50	140		70	
19	50	100	80	20	0
20	60	70		50	
11–20*		66 ± 39†		21 ± 57‡	
21	70	100		90	
22	70	60		60	
23	70	160		50	
24	75	50		0	
25	80	300		160	
26	80	120	0	180	20
27	80	350	70	160	30
28	80	50	20	20	40
29	85	140	−40	50	−60
30	85	600	60	320	10
31	85	50		110	
32	85	380	§	320	10
33	90	200		100	
34	90	90		180	
35	90	170		280	
36	90	510	800		
37	90	350		180	
21–37*		216 ± 170†		180 ± 187‡	
38	95	§		70	
39	95	§	0	130	4
40	95	220	40	80	20
38–40*		220		93 ± 32	

*Data are the mean or the mean ± standard deviation.
†P < .05.
‡P < .05.
§No signal.

DSLA Before and After Treatment of Carotid Stenosis

Ten patients with high-grade extracranial carotid stenoses underwent DSLA before and after treatment (carotid endarterectomy in six, stent angioplasty in fur). Figure 7 presents the image series and signal intensity-time courses in the CS a patient before and after endarterectomy. One patient (patient 32) had occlusion after the intervention. All other patients had dramatically reduced delays after treatment, but three had a CS ATD of more than 60 ms. Postinterventional ATDs were still significantly elevated compared with those of controls.

Discussion

The phenomenon of delayed arterial arrival associated with vascular stenoses was first described in 1960s, initially in studies by using conventional angiography (22) or scintigraphy (23, 24), whereas most later studies used contrast-enhanced dynamic CT (25), echo-enhanced transcranial Doppler sonography (26), or perfusion MR imaging (3, 27), to determine tissue perfusion in the presence of stenosis. All these studies did, however, require the administration of a contrast medium. This method might alter physiologic blood flow conditions and cannot be repeated arbitrarily. DSLA avoids these problems because it does not need contrast agents. Conventional CT angiography or MRA provide little information about the dynamics of poststenotic blood flow. The temporal resolution achieved with two-dimensional projection techniques is on the order of 0.5–1 second and 2–6 seconds per volume dataset when 3D acquisition with temporal and spatial interpolation is used (28, 29). Both techniques incorporate a compromise between temporal and spatial resolution, but the image frame rate still does not suffice for precise depiction of the hemodynamic situation in the circle of Willis or in the deeper CS. DSLA requires markedly longer
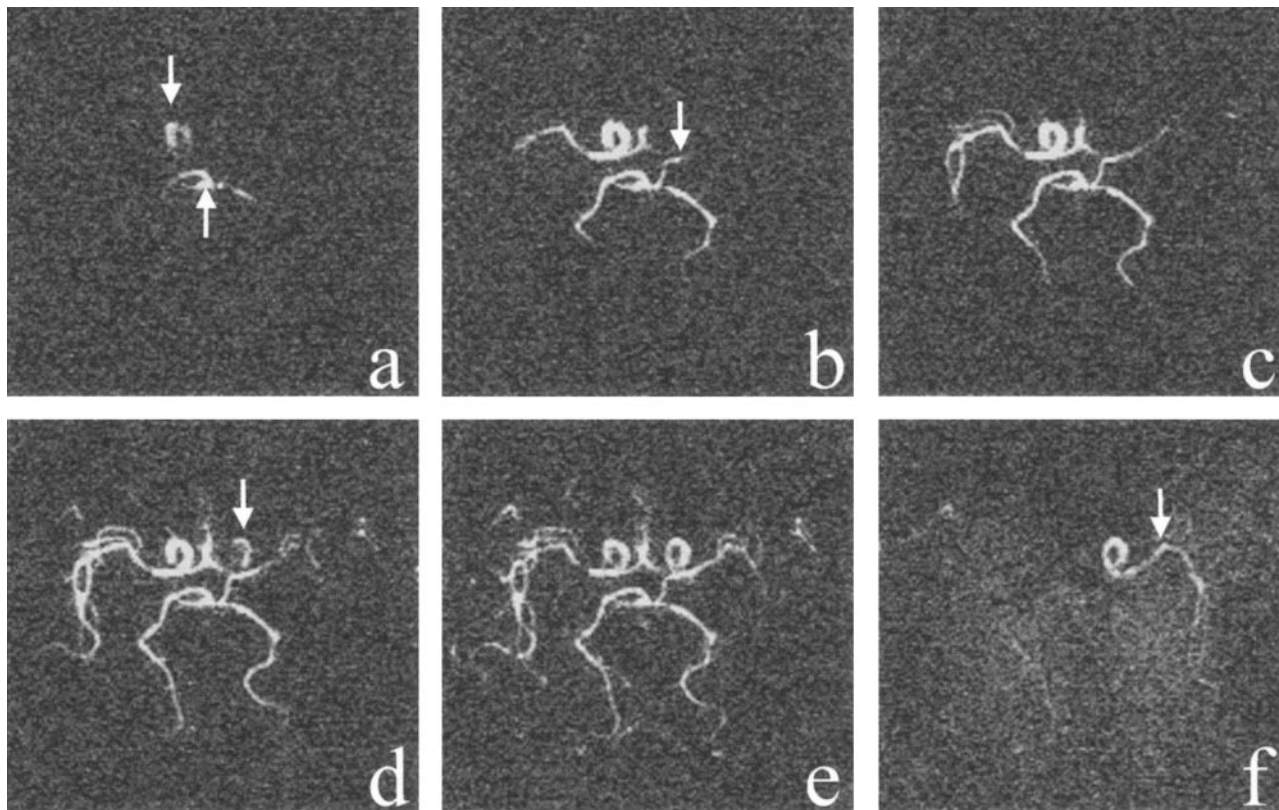
FIG 3.   Patient 30, with an 85% stenosis of the left ICA. Dynamic angiograms of the circle of Willis in foot-to-head projections at 60, 100, 140, 220, 300, and 580 ms after labeling in *a-f*. In *a*, the right ICA (*upper arrow*) and basilar artery (*lower arrow*) fill first. In *b*, Collateral flow into the left MCA via the left posterior communicating artery and the anterior communicating artery is shown. In *d*, Left ICA fills. In *f*, because of the finite length of the labeled bolus, all vessels but the left ICA and MCA contain unlabeled blood at this late phase.

FIG 4.   ATDs calculated for the CS (*left*) and MCA (*right*) increase significantly with the degree of stenosis ($P < .01$). Values at 60% and 75% stenosis are those of individual patients.
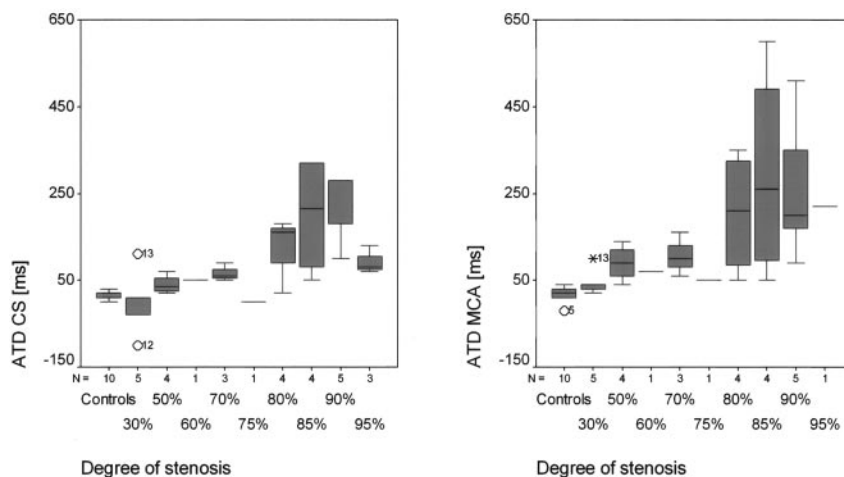
acquisition times, but it provides 10–20-fold higher temporal resolution. As opposed to DSA, the method allows for arbitrary projection directions. DSLA is not limited to being performed as a projection technique but also allows for acquiring 3D datasets. However, the increased acquisition time is no longer acceptable in clinical examinations; this limitation suggests that temporal or spatial resolution must be reduced here as well.

This study showed that the high temporal resolution of the spin labeling method makes the technique especially suitable for monitoring hemodynamic ef-

fects of stenosing cerebrovascular disease. To our knowledge, the DSLA technique presented herein is the first fully noninvasive MR imaging procedure that allows quantification of ATDs in patients with extracranial carotid stenosis. Moreover, DSLA enabled us to show the compensation of such ATDs by adequate distal collateral flow and thus provided important supplementary information on hemodynamic changes secondary to vascular stenoses.

Our results demonstrated that the degree of stenosis was best correlated with ATD in the CS. Although the proportion of stenoses <70% was small, the re-

Controls
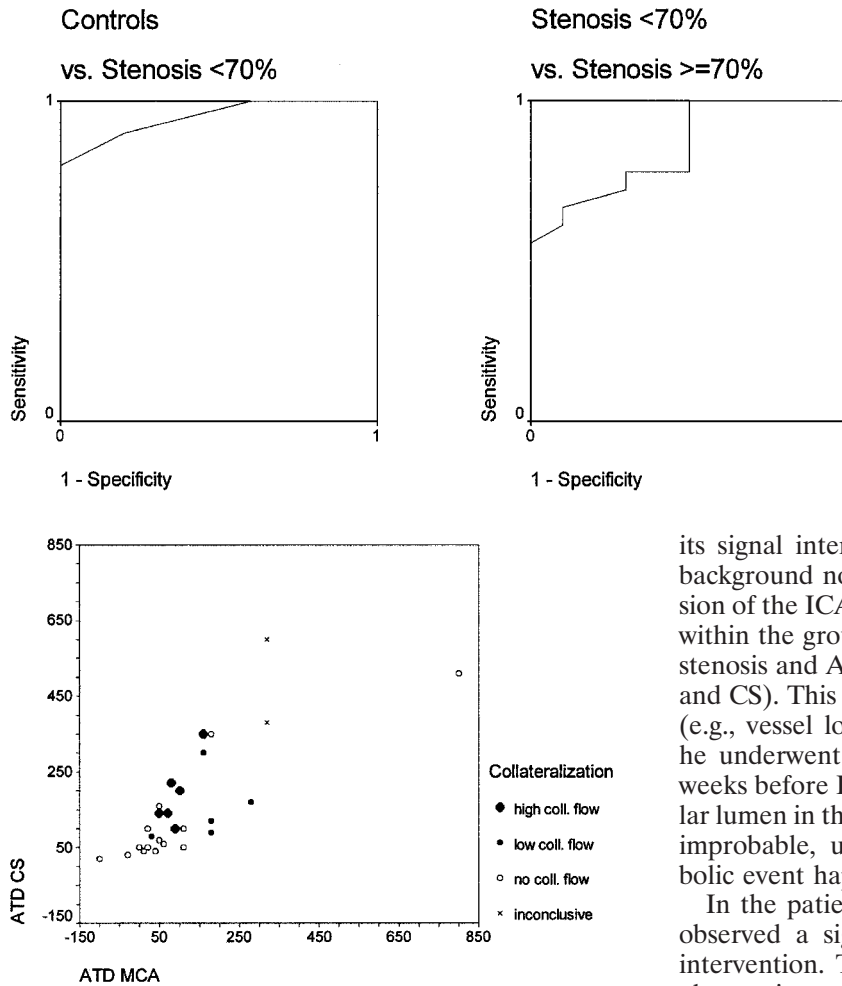### vs. Stenosis <70%

Stenosis <70%
vs. Stenosis >=70%

Fig 5. ROC curves for ATDs in the CS. *Left*, Distinction of control subjects and patients with 30–60% stenosis. *Right*, Distinction of control subjects and patients with <70% stenoses from those with 70–95% stenosis. ATD of >150 ms proved a high-grade stenosis (specificity, 100%; sensitivity, 56%).

Fig 6. Scatterplot of the ATDs calculated for the MCA versus those for the CS. Patients were subdivided by the degree of collateral flow visible on DSLA. Degree of collateralization was determined by subjectively assessing flow in the anterior and posterior communicating arteries. Patients with pronounced collateral flow are in the group in whom MCA ATD was less than CS ATD.

sults suggested that an ATD exceeding 110 ms was indicative of a stenosis of at least 70%, with a sensitivity of 67% and a specificity of 90%, or even higher specificity if control subjects and subjects with low-grade stenoses are merged in one group. All stenoses with ATD of at least 150 ms were of high grade. This additional possibility for grading vascular stenoses by using MR imaging is clinically relevant. On the basis of MRA alone, even contrast-enhanced MRA, the assessment of the degree of high-grade carotid stenoses is sometimes difficult and may lead to a misclassification of patients (30–32). Combining MRA with DSLA might significantly improve the diagnostic accuracy in such patients and furthermore reduce the necessity for conventional invasive angiography. Moreover, the technique can be used to assess the effect of treatment in patients after surgery or stent placement for ICA stenosis and to identify recurrent stenosis.

In two patients with 95% stenosis, no blood signal intensity was detected in the siphon. In both, the amount of blood was so small or it arrived so late that its signal intensity could not be distinguished from background noise; this finding suggested near-occlusion of the ICA. Large ATD variations were observed within the groups (e.g., in patient 28 who had a 30% stenosis and ATDs of more than 100 ms in the MCA and CS). This patient had no anatomic abnormalities (e.g., vessel loop) at time-of-flight MRA. However, he underwent duplex ultrasonography more than 2 weeks before DSLA. Further narrowing of the vascular lumen in the meantime to a high-degree stenosis is improbable, unless a nonsymptomatic thromboembolic event happened.

In the patients who underwent treatment, we still observed a significant transit time delay after the intervention. This result was consistent with others' observations of a considerable variability in flow velocity and its changes in the cerebral arteries of treated patients (33–35).

In addition to information on the degree of stenosis, DLSA provides information on hemodynamic changes in the brain. In 33% of patients, ATDs in the MCA are equal to or greater than those in the CS, suggesting an absence of collateralization. However, most patients had a reduced ATD distal to the circle of Willis, most probably due to collateral flow. Whether these patients have a decreased risk of cerebral ischemia remains to be determined in further studies. Of interest, patients with stenoses ≥95% had relatively early MCA filling and thus small ATDs comparable to those of patients with intermediate-grade ICA stenosis. This observation was attributed to a well-developed collateralization and may explain why patients with near-occlusion hardly benefit from intervention (36). Although thromboembolic events secondary to atherosclerotic wall processes play a role in most patients with stroke, a hemodynamic infarct pattern can be detected in up to 50% of patients with high-grade ICA stenosis (37). For this subset of patients, it seems to be important to have methods that allow us to quantify the hemodynamic effect of ICA stenosis. In acute ischemia, this could be of great diagnostic value. DSLA can potentially help in visualizing the complex postischemic vascular reaction.
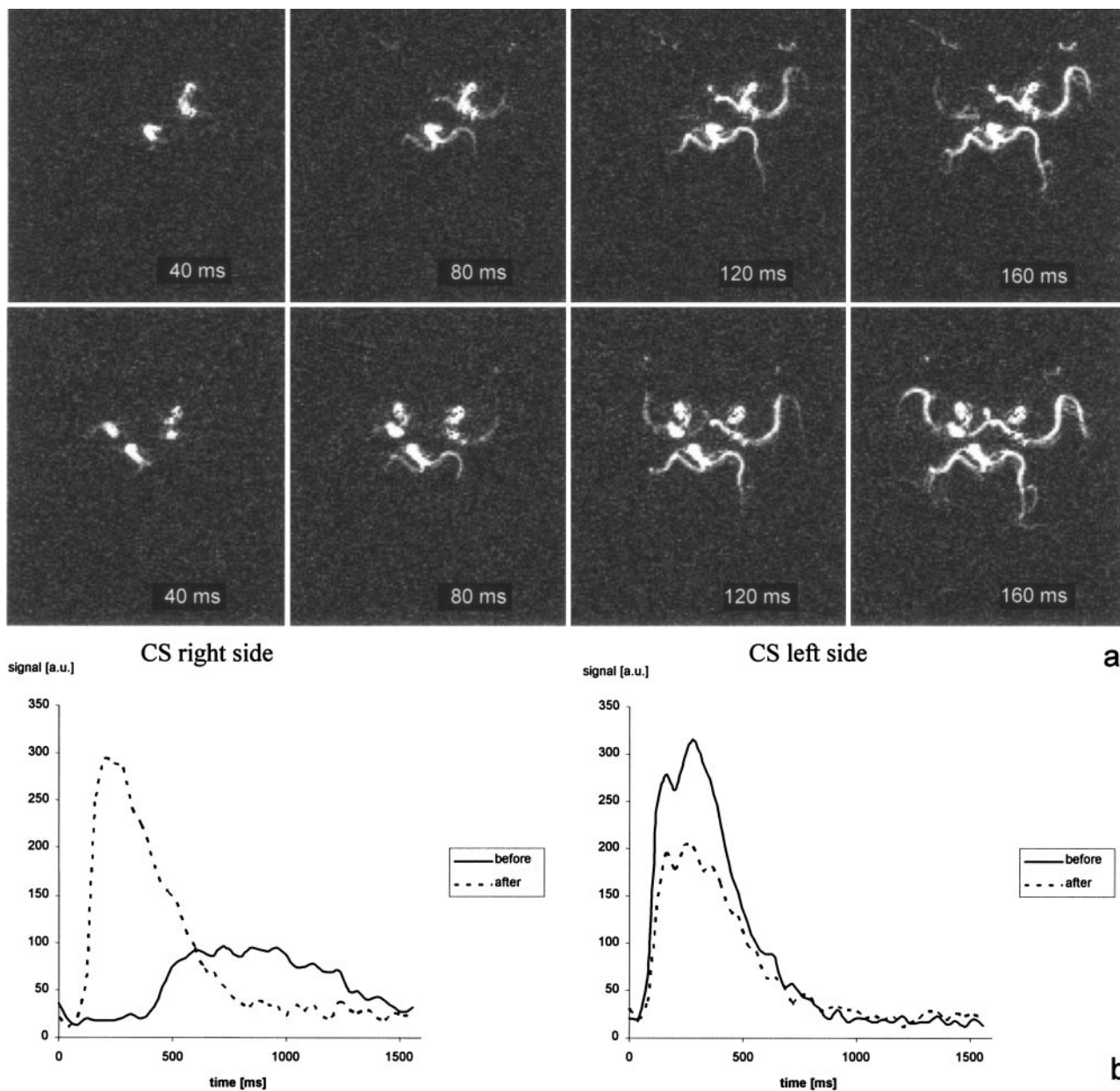
FIG 7.   In *a*, DSLA difference images of the circle of Willis in patient 40, with a 95% stenosis before and after endarterectomy. In *b*, Signal intensity–time courses in the CS. After intervention, arrival time on the affected side was the same as on that the unaffected side (about 125 ms). Amplitudes were not calibrated; hence, higher signal intensity was not associated with higher blood flow or blood volume in a vessel.

A significant limitation of our method was the inability to assess the degree of bilateral carotid stenoses, which occurred in more than 30% of patients. Determination of absolute blood arrival times in these patients is equivalent to measuring flow velocity in the vessels. However, the analysis of these absolute values gave no statistically significant results in our study. This shows that a differential method is more sensitive, as it is less dependent on section positioning. Nevertheless DSLA depicts collateralization in patients with bilateral disease as well. Having said that, in practice, patients with unilateral carotid artery stenoses can be identified with a high level of certainty by using conventional MRA, which has a high

negative predictive value (1, 38, 39). However, a restriction is that DSLA cannot be performed after the administration of contrast agent.

The greatest disadvantage of all spin labeling techniques is their poor signal-to-noise ratio, which markedly improves at high magnetic field strength (e.g., 3T). The gain for spin-labeling techniques is twofold: Magnetization in thermal equilibrium, and thus the signal intensity is higher, and decay of the magnetic label is slower. T1 relaxation time of blood is about 1650 ms at 3T compared with about 1200 ms at 1.5 T. The wider availability of MR imagers with high field strength provides new options for the use of spin labeling techniques. The FLASH readout we used to

perform DSLA does not yield optimal results in terms of signal-to-noise ratio. Double that ratio could be achieved by using segmented spiral readout at identical acquisition time and temporal resolution (40).

Conclusion

DSLA is an auspicious method for noninvasively quantifying the hemodynamic effect of an extracranial carotid artery stenosis and the resulting intracranial collateralization. It cannot replace morphologic MRA, but it may serve as a supplementary examination to enhance specificity in grading carotid artery stenoses, to monitor patients after intervention, and to provide additional functional information.

References

1. Nederkoorn PJ, van der Graaf Y, Hunink MG, et al. **Duplex ultrasound and magnetic resonance angiography compared with digital subtraction angiography in carotid artery stenosis: a systematic review.** *Stroke* 2003;34:1324–1332

2. Guckel FJ, Brix G, Schmiedek P, et al. **Cerebrovascular reserve capacity in patients with occlusive cerebrovascular disease: assessment with dynamic susceptibility contrast-enhanced MR imaging and the acetazolamide stimulation test.** *Radiology* 1996;201:405–412

3. Reith W, Heiland S, Erb G, Benner T, Forsting M, Sartor K. **Dynamic contrast-enhanced T2*-weighted MRI in patients with cerebrovascular disease.** *Neuroradiology* 1997;39:250–257

4. Rutgers DR, Klijn CJ, Kappelle LJ, van Huffelen AC, van der Grond J. **A longitudinal study of collateral flow patterns in the circle of Willis and the ophthalmic artery in patients with a symptomatic internal carotid artery occlusion.** *Stroke* 2000;31:1913–1920

5. Bendszus M, Koltzenburg M, Burger R, Warmuth-Metz M, Hoffmann E, Solymosi L. **Silent embolism in diagnostic cerebral angiography and neurointerventional procedures: a prospective study.** *Lancet* 1999;354:1594–1597

6. Williams DS, Detre JA, Leigh JS, Koretsky AP. **Magnetic resonance imaging of perfusion using spin inversion of arterial water.** *Proc Natl Acad Sci U S A* 1992;89:212–216

7. Wong EC, Buxton RB, Frank LR. **Quantitative Imaging of perfusion using a single substraction (QUIPSS and QUIPSS II).** *Magn Reson Med* 1998;39:702–708

8. Dixon WT, Du LN, Faul DD, Gado M, Rossnick S. **Projection angiograms of blood labeled by adiabatic fast passage.** *Magn Reson Med* 1986;3:454–462

9. Nishimura DG, Macovski A, Pauly JM, Conolly SM. **MR angiography by selective inversion recovery.** *Magn Reson Med* 1987;4:193–202

10. Roberts DA, Bolinger L, Detre JA, Insko EK, Bergey P, Leigh JS Jr. **Continuous inversion angiography.** *Magn Reson Med* 1993;29:631–636

11. Wang SJ, Nishimura DG, Macovski A. **Fast angiography using selective inversion recovery.** *Magn Reson Med* 1990;23:109–121

12. Wang SJ, Nishimura DG, Macovski a. **Multiple-readout selective inversion recovery angiography.** *Magn Reson Med* 1991;17:244–251

13. Edelman RR, Siewert B, Darby DG, et al. **Qualitative mapping of cerebral blood flow and functional localization with echo-planar MR imaging and signal targeting with alternating radio frequency.** *Radiology* 1994;192:513–520

14. Detre JA, Leigh JS, Williams DS, Koretsky AP. **Perfusion imaging.** *Magn Reson Med* 1992;23:37–45

15. Kim SG. **Quantification of relative cerebral blood flow change by flow-sensitive alternating inversion recovery (FAIR) technique: application to functional mapping.** *Magn Reson Med* 1995;34: 293–301

16. Kwong KK, Chesler DA, Weisskoff RM, et al. **MR Perfusion Studies with T1-Weighted Echo Planar Imaging.** *Magn Reson Med* 1995;34:878–887

17. Look D, Locker D. **Time saving in measurement of NMR and EPR relaxation times.** *Rev Sci Instrum* 1970;41:250–251

18. Gunther M, Bock M, Schad LR. **Arterial spin labeling in combination with a look-locker sampling strategy: inflow turbo-sampling EPI-FAIR (ITS-FAIR).** *Magn Reson Med* 2001;46:974–984

19. **Clinical alert: benefit of carotid endarterectomy for patients with high-grade stenosis of the internal carotid artery.** *Stroke* 1991;22:816–817

20. **MRC European Carotid Surgery Trial: interim results for symptomatic patients with severe (70–99%) or with mild (0–29%) carotid stenosis—European Carotid Surgery Trialists' Collaborative Group.** *Lancet* 1991;337:1235–1243

21. Rothwell PM, Gibson RJ, Slattery J, Sellar RJ, Warlow CP. **Equivalence of measurements of carotid stenosis: a comparison of three methods on 1001 angiograms—European Carotid Surgery Trialists' Collaborative Group.** *Stroke* 1994;25:2435–2439

22. Boczko ML, Caplan LH. **Alteration of flow dynamics in the carotid artery system of "stroke" patients: clinical and arteriographic study.** *Invest Radiol* 1967;2:33–40

23. Oldendorf WH, Crandall PH, Nordyke RA, Rose AS. **A comparison of the arrival in the cerebral hemispheres of intravenously injected radioisotope: a preliminary report.** *Neurology* 1960;10:223–227

24. Tolonen U. **Quantitative 99mTechnetium cerebral circulation time in brain infarction. Its relation to clinical findings, electroencephalograms and conventional radionuclide studies.** *Acta Neurol Scand* 1981;5:337–352

25. Davis SM, Tress BM, Hopper JL, Kaye AH, Rossiter SC. **Dynamic CT brain scanning in the haemodynamic evaluation of cerebral arterial occlusive disease.** *Neuroradiology* 1987;29:259–265

26. Schreiber S, Weih M, Hofmann O, Rückert R, Einhäupl KM, Valdueza JM. **Delayed transcranial echo-contrast bolus arrival in carotid artery disease.** In: Proceedings of the 4th Meeting of the European Society of Neurosonology and Cerebral Hemodynamics. 1999:48

27. Nighoghossian N, Berthezene Y, Philippon B, Adeleine P, Froment JC, Trouillas P. **Hemodynamic parameter assessment with dynamic susceptibility contrast magnetic resonance imaging in unilateral symptomatic internal carotid artery occlusion.** *Stroke* 1996;27: 474–479

28. Wang Y, Johnston DL, Breen JF, et al. **Dynamic MR digital subtraction angiography using contrast enhancement, fast data acquisition, and complex subtraction.** *Magn Reson Med* 1996;36:551–556

29. Korosec FR, Frayne R, Grist TM, Mistretta CA. **Time-resolved contrast-enhanced 3D MR angiography.** *Magn Reson Med* 1996;36: 345–351

30. Johnston DCC, Eastwood JD, Nguyen T, Goldstein LB. **Contrast-enhanced magnetic resonance angiography of carotid arteries: utility in routine clinical practice.** *Stroke* 2002;33:2834–2838

31. Patel SG, Collie DA, Wardlaw JM, et al. **Outcome, observer reliability, and patient preferences if CTA, MRA, or Doppler ultrasound were used, individually or together, instead of digital subtraction angiography before carotid endarterectomy.** *J Neurol Neurosurg Psychiatry* 2002;73:21–28

32. Wardlaw JM, Lewis SC, Humphrey P, Young G, Collie D, Warlow CP. **How does the degree of carotid stenosis affect the accuracy and interobserver variability of magnetic resonance angiography?** *J Neurol Neurosurg Psychiatry* 2001;71:155–160

33. Araki CT, Babikian VL, Cantelmo NL, Johnson WC. **Cerebrovascular hemodynamic changes associated with carotid endarterectomy.** *J Vasc Surg* 1991;13: 854–859

34. Vriens EM, Wieneke GH, Hillen B, Eikelboom BC, Van Huffelen AC, Visser GH. **Flow redistribution in the major cerebral arteries after carotid endarterectomy: a study with transcranial Doppler scan.** *J Vasc Surg* 2001;33:139–147

35. Blohme L, Pagani M, Parra-Hoyos H, Olofsson P, Takolander R, Swedenborg J. **Changes in middle cerebral artery flow velocity and pulsatility index after carotid endarterectomy.** *Eur J Vasc Surg* 1991;5:659–663

36. Rothwell PM, Eliasziw M, Gutnikov SA, et al. **Analysis of pooled data from the randomised controlled trials of endarterectomy for symptomatic carotid stenosis.** *Lancet* 2003;361:107–116

37. Szabo K, Kern R, Gass A, Hirsch J, Hennerici M. **Acute stroke patterns in patients with internal carotid artery disease: a diffusion-weighted magnetic resonance imaging study.** *Stroke* 2001;32: 1323–1329

38. Wolfle KD, Schnur C, Pfadenhauer K, Bruijnen H, Bohndorf K, Loeprecht H. **MR-angiography and duplex-ultrasonography: predictive reliability for angiographically determined internal carotid artery stenosis >/= 70–99%.** *Zentralbl Chir* 2002;127:81–88

39. Tiev KP, Sevestre MA, Reix T, et al. **Quantitative assessment of carotid stenosis: comparison between Doppler ultrasound, spiral computed tomography angiography, magnetic resonance angiography and digital angiography.** *J Mal Vasc* 2000;25:325–331

40. Amann M, Warmuth C, Günther M, Zimmer C, Schad LR. **Dynamic spin labeling cerebral 2-D angiography: a comparison between FLASH and spiral readout.** In: *Proceedings of the International Society for Magnetic Resonance in Medicine.* Berkeley, CA: International Society for Magnetic Resonance in Medicine; 2002: 629